0026-895X/96/040770-11$3.00/0

MOLECULAR PHARMACOLOGY, 50:770–780 (1996).

Ligand-Binding Characteristics and Related Structural Features of the Expressed Goldfish Kainate Receptors: Identification of a Conserved Disulfide Bond and Three Residues Important for Ligand Binding

Z. GALEN WO and ROBERT E. OSWALD

Department of Pharmacology, College of Veterinary Medicine, Cornell University, Ithaca, New York 14853

Received April 1, 1996; Accepted June 8, 1996

SUMMARY

Low-molecular-weight kainate receptors from nonmammalian vertebrate brain belong structurally to the ionotropic glutamate receptor superfamily. In this study, two previously cloned goldfish kainate receptor subunits (GFKARα and GFKARβ) were transiently expressed in human embryonic kidney 293 cells, and their ligand-binding properties and some associated structural features were characterized, resulting in the following findings. 1) Both subunits form homomeric receptors with high affinity for [^{3}H]kainate (K_D = 16 and 31 nM, respectively) and L-glutamate (K_D = 2 and 40 μM, respectively). 2) A deletion mutant lacking the originally proposed second-transmembrane domain was efficiently expressed and retains the overall ligand-binding properties of wild-type GFKARα, strongly indicating that this region is not a transmembrane domain. 3) Mutations of Q12, A53, and Y54 of GFKARβ indicate that these three residues are important for ligand binding (particularly L-glutamate), which is consistent with the sequence homology to bacterial periplasmic binding proteins. 4) Mutation of the three extracellular cysteine residues of GFKARβ indicated that the two conserved cysteine residues (C305 and C385), located between two transmembrane segments, form a solvent-accessible disulfide bond. Analysis of [^{3}H]kainate binding to wild-type and cysteine mutations of GFKARβ indicate that in the absence of the disulfide bond, the affinity for kainate is increased 3-fold. These data lend further evidence in support of a model of glutamate receptor topology with three transmembrane segments and reveal several general structural features of the extracellular ligand-binding domain of the kainate receptors. These results are consistent with the notion that the ligand-binding domain has close structural similarities to bacterial periplasmic binding proteins.

Glutamate is the principal excitatory neurotransmitter in the vertebrate central nervous system. The iGluRs, which form ligand-gated ion channels, are divided into AMPA, kainate, and NMDA subtypes based on pharmacological and electrophysiological criteria (1). Intensive effort has been focused on cloning and functional characterization of iGluRs from mammalian species (molecular mass, ≥100 kDa) and has revealed the complexity and diversity of the iGluR superfamily (2–4). AMPA receptors consist of GluR1-4 subunits, and kainate receptors consist of GluR5-7 and KA-1 and KA-2 subunits. NMDA receptors are formed by NR1 and NR2A–2D subunits. Functional ion channels are formed by subunits of 100 kDa either alone or in various combinations within each of the above three subclasses. In addition, the iGluR superfamily includes the "orphan" receptors GluRδ1 and GluRδ2 (5). Although no ion channel activity has been observed for these receptors, results from transgenic mice carrying a mutant form of GluRδ2 indicates their physiological importance (6). Limited molecular cloning work also shows that the brains of nonmammalian vertebrate species express AMPA (7, 8) and NMDA (9) iGluRs that are remarkably homologous (>95% identity) to the cloned mammalian counterparts.

Kainate, a cyclic analog of L-glutamate, has been used extensively for characterization of the kainate subclass of

This work was supported by grants from the National Science Foundation (IBN-9309480) and the John Simon Guggenheim Memorial Foundation (R.E.O.). Z.G.W. was supported by a Pharmaceutical Research and Manufacturers of America Foundation Advanced Predoctoral Fellowship.

ABBREVIATIONS: iGluR, ionotropic glutamate receptor; GluR, glutamate receptor; AMPA, α-amino-3-hydroxy-5-methyl-4-isoxazolepropionic acid; CNQX, 6-cyano-2,3-dihydroxy-7-nitroquinoxaline; KBP, kainate-binding protein; GFKARα, 45-kDa kainate receptor subunit from goldfish brain; GFKARβ, 41-kDa kainate receptor subunit from goldfish brain; HEK, human embryonic kidney; NMDA, *N*-methyl-D-aspartate; SDS-PAGE, sodium dodecyl sulfate-polyacrylamide gel electrophoresis; TMI, first putative transmembrane domain; TMII, second putative transmembrane domain; TMIII, third putative transmembrane domain; TMIV, fourth putative transmembrane domain; HBP, histidine-binding protein; DTT, dithiothreitol; DTNB, 5,5′-dithio-bis(2-nitrobenzoic acid); GSSG, oxidized glutathione; NEM, *N*-ethylmaleimide.

glutamate receptors. Nonmammalian vertebrate brain has a much higher density of high affinity kainate binding sites than mammals, and kainate receptor proteins of ~50 kDa have been purified and characterized biochemically from frog, chick, and goldfish brains (10–12). These kainate receptor proteins (also known as KBPs) cloned from nonmammalian species (i.e., fish, frog, and bird; Refs. 13–16) are homologous to the carboxyl-terminal half of subunits (~100 kDa) of AMPA and kainate receptors, and the homology is the highest (~40%) with the GluR6 kainate receptor. Cytochemical analysis with specific antibodies (17, 18) or [^{3}H]kainate as a probe (19) on fish, frog, and chick brains and *in situ* hybridization of chick brain (20) showed that these kainate receptors are predominantly expressed in the cerebellum of brain, particularly in Bergmann glial cells of the molecular layer.

Recently, it has become increasingly clear that members of the iGluR superfamily share common structural features that are distinct from those of other ligand-gated ion channels. Topological analysis of the 50-kDa kainate receptors (15, 21, 22) and 100-kDa AMPA and NMDA receptors (23, 24) revealed that the subunits of these integral membrane proteins have three transmembrane segments (initially designated TMI, TMIII, and TMIV, as originally defined by hydropathy plots), whereas the key segment previously termed TMII is not a true transmembrane segment and probably forms a loop that forms a portion of the channel pore. The TMII region is related to the channel pore region of voltage-gated K^+ channels (25, 26). The two large extracellular domains predicted by the three-transmembrane domain model share significant sequence homology with bacterial amino acid-binding proteins (27, 28) and are likely to be involved in ligand binding because ligand-binding specificity is determined in part by residues in the second extracellular loop (29, 30). Thus, ionotropic AMPA and kainate receptors as well as the closely related nonmammalian kainate receptors seem to be modular proteins that are constructed from several ancient structural elements (25). Structural models for the extracellular ligand-binding domain and the transmembrane channel portion of non-NMDA receptors have been produced through the use of homologous modeling (31).

In this study, we obtained transient expression of the two cloned goldfish brain kainate receptors in HEK 293 cells and characterized the biochemical and pharmacological properties of the expressed receptor proteins. In addition, mutational analysis revealed structural features of the extracellular domains that form the ligand-binding site, and we provide further evidence to support a three-transmembrane topology model for these receptor proteins. This study also shows that these two kainate receptors bind to L-glutamate with physiologically significant affinity, which may play an important role in the synaptic transmission in the brain of nonmammalian vertebrates.

Experimental Procedures

Materials. [^{3}H]Kainic acid (60 Ci/mmol) and autoradiography enhancer INTENSIFY were purchased from DuPont-New England Nuclear (Boston, MA). *N*-Glycosidase F was obtained from Boehringer-Mannheim (Indianapolis, IN). The monoclonal antibody KAR-B1 was a gift from Dr. David R. Hampson (University of Toronto, Ontario, Canada). Polyclonal antipeptide antiserums Ab-α1 against GFKARα and Ab-β1 against GFKARβ were produced by Research Genetics (Huntsville, AL) (21). Glutamatergic ligands AMPA, CNQX, domoate, and quisqualate were purchased from Research Biochemicals (Natick, MA). thioreactive agents DTT, NEM, GSSG, and DTNB were purchased from Sigma Chemical (St. Louis, MO). cDNA sequencing was performed by the Cornell DNA Sequencing Facility (Ithaca, NY).

Expression in cultured HEK 293 cells. To transfect HEK 293 cells, cDNAs were subcloned from pcDNAII vector into the expression vector pRBG4 (32). HEK 293 cells, grown to 6×10^5 cells/10-cm dish, were transfected (20 μg of plasmid DNA/dish) using the calcium phosphate precipitation method, and cell membranes were prepared 48 hr after transfection as described previously (21). Membrane pellets from each dish were resuspended in 0.5 ml (~1 mg of protein/ml) of 1 mM phenylmethylsulfonyl fluoride and stored at −20°. Each binding assay contained 4–8 μg of protein.

Gel electrophoresis and immunoblotting. As described previously (21), samples (4–8 μl) of transfected HEK 293 cell membrane preparations were solubilized in SDS loading buffer (8% β-mercaptoethanol) and separated by 10% SDS-PAGE. Proteins were electrophoretically transferred from the gel to an Immobilon-P membrane (Millipore, Bedford, MA). Membranes were blotted sequentially using either monoclonal antibody FKAR-B1 or the specific anti-peptide antibodies (Ab-α1 and Ab-β1; Ref. 21) followed by a second antibody (horseradish peroxidase-conjugated goat anti-mouse IgG). Proteins recognized by the monoclonal antibody FKAR-B1 were visualized using Renaissance chemiluminescence reagent (DuPont-New England Nuclear).

[^{3}H]Kainate-binding assay. [^{3}H]Kainate binding to membrane fragments of goldfish cerebellum and transfected cells was measured as described previously for membranes (33, 34). The additional presence of 100 μM kainate in the assays defined nonspecific binding. Equilibrium binding was analyzed by a nonlinear fit to the Hill equation ($[RL] = B_{max}[L]^{nH}/(K_D^{nH} + [L]^{nH})$, where n_H is the Hill coefficient, $[RL]$ is the concentration of bound ligand, and $[L]$ is the concentration of free ligand). The K_D values reported below correspond to the K_D value given in this equation, which corresponds to the concentration of free ligand at half-maximal saturation (K_D values are reported with standard errors of three or four independent observations). To obtain the binding profiles of glutamatergic agonists and an antagonist (CNQX), [^{3}H]kainate binding displacement assays were done with 15–25 nM [^{3}H]kainate and the test compounds at indicated concentrations (three observations for L-glutamate inhibition and two observations for all others). Incubations were carried out for 1 hr on ice, and the mixtures were filtered through glass-fiber filters (Schleicher & Schuell, Keene, NH) and washed once. The K_I value was calculated from the IC_{50} value using the Cheng-Prusoff equation (35) modified to include kainate cooperativity where appropriate $\{K_I = IC_{50}/[1 + (L^{nH}/K_D^{nH})]\}$. The amount of nonspecific binding was determined by the inclusion of excess nonradioactive kainate.

[^{3}H]Kainate dissociation rate measurements. Goldfish cerebellum (the brain region containing the highest concentration of [^{3}H]kainate-binding sites; Ref. 19) or membranes from transfected HEK 293 cells were incubated in the presence or the absence of 2 mM DTT for 10 min at room temperature. Treatment of membranes with DTT for longer periods had no additional effects. For dissociation measurements, [^{3}H]kainate was added to a final concentration of 30 nM. The binding mixture was incubated for 1 hr on ice. Unlabeled kainate was then added to a final concentration of 1 mM, and the suspension was mixed thoroughly. Samples (0.5 ml for goldfish cerebellum or 150 μl for transfected HEK 293 cell membranes) were removed at appropriate times and filtered through Schleicher & Schuell glass-fiber filters. The amount of bound [^{3}H]kainate was determined as described above.

Construction of mutants and expression vectors. The overlapping PCR method was used to generate eight single-point and one double mutation of GFKARβ. A silent mutation, creating a new restriction site for analysis, was introduced with each point-mutation to facilitate the identification of mutant clones. The overlapping

primer pairs used were 5′-CCATCAAGGAAGACCC-3′ (sense) and 5′-GGGTCTTCCTTGATGG-3′ (antisense) for β(Q12E), 5′-GATGGAAAGTATGGCCGGCAG-3′ (sense) and 5′-TGCCGGCCATACTTTCCATCC-3′ (antisense) for β(A51K), 5′-GGAGCGTTTGGCCGGCAG-3′ (sense) and 5′-CTGCCGGCCAAACGCTCC-3′ (antisense) for β(Y52F), 5′-GGAGCGGCTGGCCGGCAG-3′ (sense) and 5′-CTGCCGGCCAGCCGCTCC-3′ (antisense) for β(Y52S), 5′-GGCTACTCCATGGATCTG-3′ (sense) and 5′-GATCCATGGAGTAGCC-3′ (antisense) for β(C27S), 5′-CGCCATTCTGAGCTCGTCCG-3′ (sense) and 5′-GACGAGCTCAGAATGGCGTG-3′ (antisense) for β(C305S), and 5′-GGCCAGCTCGAGTATACCG-3′ (sense) and 5′-GGTATACTCGAGCTGGCCCA-3′ (antisense) for β(C358S). The six PCR fragments, containing either the Q12E, A51K, Q12E/A51K, Y52F, Y52S, or C27S mutation, were cut with *Bam*HI and *Eco*RV, and the resulting cassettes of 400 bp were purified and exchanged for the respective fragments of wild-type GFKARβ cDNA in the pRBG4 vector. Two PCR products containing the C305S and C358S mutations were cut with *Eco*RV and *Acc*I, and the resulting cassettes of 700 bp were exchanged for the respective wild-type fragments of GFKARβ cDNA. A total of eight cDNAs with the above point-mutations were transferred into the expression vector for transfection of HEK 293 cells. The PCR products containing mutations were verified by DNA sequencing. In the case of αΔTMII, a previously constructed deletion mutant (15), the cDNA insert (2 kb) in pcDNAII vector was subcloned into the expression vector pRBG4.

Results

Expression of GFKARα and GFKARβ in transfected HEK 293 cells. To express goldfish kainate receptor subunits *in vivo* for structural and functional characterization, HEK 293 cells were transfected with GFKARα and GFKARβ cDNAs in the expression vector pRBG4 by the Ca^{2+}/phosphate precipitation method. Both GFKARα and GFKARβ proteins were efficiently expressed as indicated by Western blotting (Fig. 1) with the monoclonal antibody FKAB-B1 (36). FKAB-B1 was raised against frog KBP but recognizes GFKARα (45 kDa) and GFKARβ (41 kDa) as well (22). When the same amount of GFKARα and GFKARβ cDNA was used for cotransfection, the expression of GFKARβ was slightly higher (~1.5-fold) than that of GFKARα, based on the Western blot (Fig. 1A, *lane 4*). The GFKARα and GFKARβ proteins have the same number of amino acids (439 amino acids; Ref. 15), and the difference in apparent molecular mass seems to be due to *N*-glycosylation because treatment of the membranes with *N*-glycosidase F produces a single band of ~40 kDa (22). The difference in molecular mass (~4 kDa) of the fully glycosylated forms of GFKARα and GFKARβ is entirely consistent with previous studies (15, 21) using *in vitro* translation that demonstrated that GFKARα has three functional *N*-glycosylation sites (N307, N333, and N340) and GFKARβ has only one (N332). In the case of GFKARα, two glycosylated forms are observed: one with two of the sites glycosylated and one with three of the sites glycosylated (21). For both GFKARα and GFKARβ, the nonglycosylated forms produced either by *in vitro* translation in the absence of microsomal membranes or by enzymatic digestion with *N*-glycosidase F exhibited an apparent molecular mass (40 kDa) that was somewhat smaller than predicted from the amino acid sequence (48 kDa), possibly due to the presence of several hydrophobic segments in the sequence. The migration pattern was identical in the presence and absence of reducing agents (data not shown).

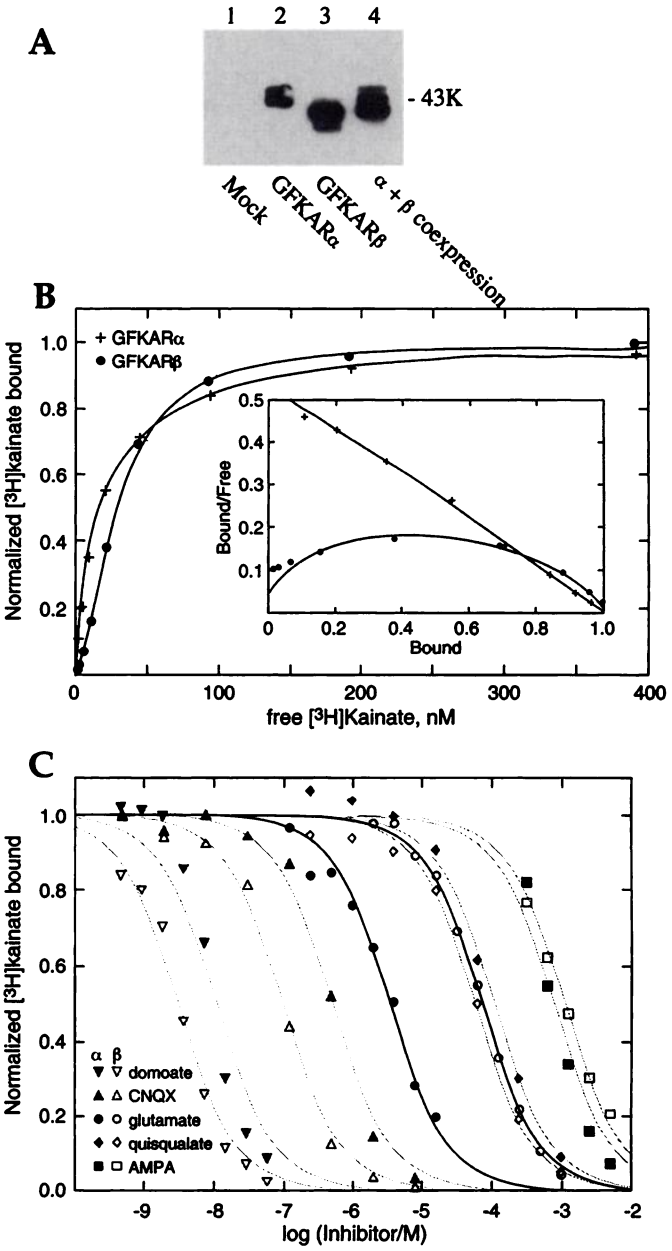

Fig. 1. A, Immunoblot of proteins extracted from HEK 293 cells transfected with GFKARα and GFKARβ cDNA. Samples of the transfected cell membrane preparations were subjected to SDS-PAGE, transferred to Immobilon-P membranes, probed with a monoclonal antibody (KAR-B1), and visualized by chemiluminescence. B, Equilibrium binding of [^{3}H]kainate to homomeric receptors formed from wild-type goldfish kainate receptor subunits (GFKARα and GFKARβ) expressed in HEK 293 cells. *Inset*, Scatchard plots of the saturation data. The maximal binding corresponds to 10–20 pmol/mg of protein. C, Comparison of the competitive inhibition of [^{3}H]kainate binding to goldfish kainate receptors expressed in HEK 293 cells. The membrane preparations were incubated with 20 nM [^{3}H]kainate and increasing concentrations of the glutamate analogs domoate, glutamate, quisqualate, AMPA, and CNQX. The results are presented as a percentage of binding the absence of inhibitor. See Table 1 for the K_i values calculated from the IC_{50} values.

Ligand-binding properties of GFKARα and GFKARβ in HEK 293 cells. The binding of [^{3}H]kainate to GFKARα and GFKARβ receptors expressed in HEK 293 cells was specific and saturable, with K_D values of 16 ± 3 and 31 ± 3 nM, respectively (Fig. 1B). The binding of [^{3}H]kainate to

GFKARβ was positively cooperative (n_H = 1.8 ± 0.1), whereas GFKARα displayed little or no cooperativity (n_H = 1.1 ± 0.1). Likewise, native kainate receptors from goldfish brain bind kainate with a K_D value of ~30 nM and show some positive cooperativity (37). Displacement profiles for several glutamate analogs (Fig. 1C) showed that GFKARα and GFKARβ have similar affinities for domoate, CNQX, quisqualate, and AMPA (Table 1). Interestingly, GFKARα and GFKARβ have significantly different affinities for L-glutamate (IC_{50} = 3.2 ± 0.3 and 71.4 ± 0.5 μM, respectively, at 25 nM [^{3}H]kainate and 4°; Fig. 1C). Based on calculation of the K_I value with the Cheng-Prusoff equation (corrected for cooperativity), GFKARα binds L-glutamate with an affinity that is 30-fold greater than that of GFKARβ (Table 1). GFKARα and GFKARβ coexpressed in HEK 293 cells exhibit an IC_{50} value of 32 μM for L-glutamate, which is approximately the value obtained for native kainate receptors (α and β mixed) from goldfish brain (33, 37). Thus, the ligand-binding characteristics of GFKARα and GFKARβ expressed in HEK 293 cells are in good agreement with the overall ligand-binding properties previously measured on the native receptors from goldfish brain, which are an approximately equal mixture of the two subunits (12). In addition, ligand binding was measured at 20°. The affinity of GFKARα was decreased 2-fold for the agonists kainate and L-glutamate and decreased ~6-fold for the antagonist CNQX (Table 1). On the other hand, the affinity of GFKARβ for kainate and L-glutamate was slightly increased at 20° versus 4°, whereas its affinity for the antagonist CNQX was decreased 6-fold (Table 1). To maintain consistency with previously published experiments, all ligand-binding assays in the following sections were carried out at 4°.

Expression and characterization of a deletion mutant, αΔTMII. Our previous topological analysis of GFKARα in an *in vitro* translation/membrane translocation system showed that deletion of TMII of GFKARα (αΔTMII) has no effect on the glycosylation of sites between TMIII and TMIV, which indicates that the originally proposed second-transmembrane segment (TMII), unlike a true transmembrane domain, does not traverse the membrane (15). However, the coupled translation/membrane translocation is only the first step in the biosynthetic pathway of a membrane protein. To be efficiently expressed *in vivo*, a membrane protein must be able to undergo post-translational/translocational modifications and fold correctly in the endoplasmic reticulum and Golgi apparatus. We tested whether the GFKARα protein with the deletion of the TMII (total of 19 amino acid residues, FTLSHSFWYTMGAMTLQGA) could be expressed in transfected cells. The expression vector, pRBG4, containing αΔTMII cDNA was transfected into HEK 293 cells. The αΔTMII protein was recognized as a band slightly smaller than the wild-type GFKARα (43 kDa) in immunoblotting (Fig. 2A). The mutant receptor protein (αΔTMII) was *N*-glycosylated in the same manner as the wild-type GFKARα. Thus, αΔTMII was efficiently expressed in the transfected HEK 293 cells. Furthermore, [^{3}H]kainate saturation binding (Fig. 2B) showed that αΔTMII retains high affinity (K_D = 66 ± 5 nM) for [^{3}H]kainate, which is ~3-fold less than wild-type GFKARα. Thus, [^{3}H]kainate binding is sensitive to the presence of TMII, but nevertheless, the ligand-binding site seems to form correctly in this deletion mutant. To determine whether deletion of TMII changes other pharmacological characteristics, several glutamatergic ligands were tested in displacement studies of [^{3}H]kainate binding. The inhibition profiles of domoate, quisqualate, CNQX, and L-glutamate for [^{3}H]kainate binding to αΔTMII were similar to that for wild-type GFKARα (with some reduction in apparent affinity; Fig. 2C). αΔTMII also retains sensitivity to DTT (Fig. 6C), indicating that it also forms the disulfide bond found in the wild-type subunit. These results indicate that a kainate receptor subunit lacking the proposed "TMII" could be expressed in transfected mammalian cells and folded correctly to form the ligand-binding site. However, the decreased affinities for kainate and L-glutamate are interesting in light of the possible domain movement postulated to occur based on homology with bacterial amino acid-binding proteins (31). On the other hand, deletion of the carboxyl-terminal cytoplasmic tail of GFKARα did not result in any noticeable change in the ligand-binding properties.[1] A likely explanation is that deletion of TMII does not directly affect residues in contact with ligand but may affect the closure of the two extracellular lobes. It is noteworthy that although the hinge regions connecting the two lobes of bacterial binding proteins do not directly contact ligand, mutations of the hinge region can impair the hinge motion, as occurs with the S92F mutant of HBP (38).

Mutations of three residues of GFKARβ important for ligand binding. Previous mutational analysis of the AMPA receptors (39, 40) has suggested that two charged residues in two conserved sequence motifs (VTTILE and DGKYG)[2] in the amino-terminal extracellular region are important for ligand binding (Fig. 3A). Mutation of the glutamate of the VTTILE motif and the lysine of the DGKYG motif decreased L-glutamate affinity dramatically (39, 40). In case of lysine, the EC_{50} for channel activation by L-glutamate was decreased >20-fold, but the EC_{50} for kainate was unchanged (39, 40), indicating that residues may affect agonist binding

TABLE 1

Ligand-binding properties of kainate receptor subunits expressed in HEK 293 cells

K_D values were obtained for kainate from a nonlinear least-squares fit to the results of [^{3}H]kainate saturation binding assays. K_I values were calculated from [^{3}H]kainate displacement curves (Fig. 1C) using the Cheng-Prusoff equation (35), corrected where appropriate for the Hill coefficient.

Receptor	Ligand	K_D or K_I at 4°	K_D or K_I at 20°
GFKARα	Kainate	16 nM	47 nM
	Domoate[b]	4.3 nM	ND
	L-Glutamate	1.2 μM	6.7 μM
	Quisqualate	42 μM	ND
	AMPA	289 μM	ND
	CNQX	200 nM	1.7 μM
GFKARβ	Kainate[a]	31 nM	25 nM
	Domoate[b]	1.8 nM	ND
	L-Glutamate	42 μM	35 μM
	Quisqualate	35 μM	ND
	AMPA	655 μM	ND
	CNQX	60 nM	318 nM

[a] The Hill coefficient for [^{3}H]kainate binding to GFKARβ was 1.8; all other Hill coefficients were not significantly different than 1.

[b] Some depletion of domoate was present at low concentrations so that the assumptions of the Cheng-Prusoff equation were not strictly met. For this reason, the determination for domoate should be considered approximate.

[1] W. M. Byrnes and R. E. Oswald, unpublished observations.

[2] VTTILE and DGKYG are the consensus sequences for AMPA and kainate receptors. Some variability occurs at the underlined positions.

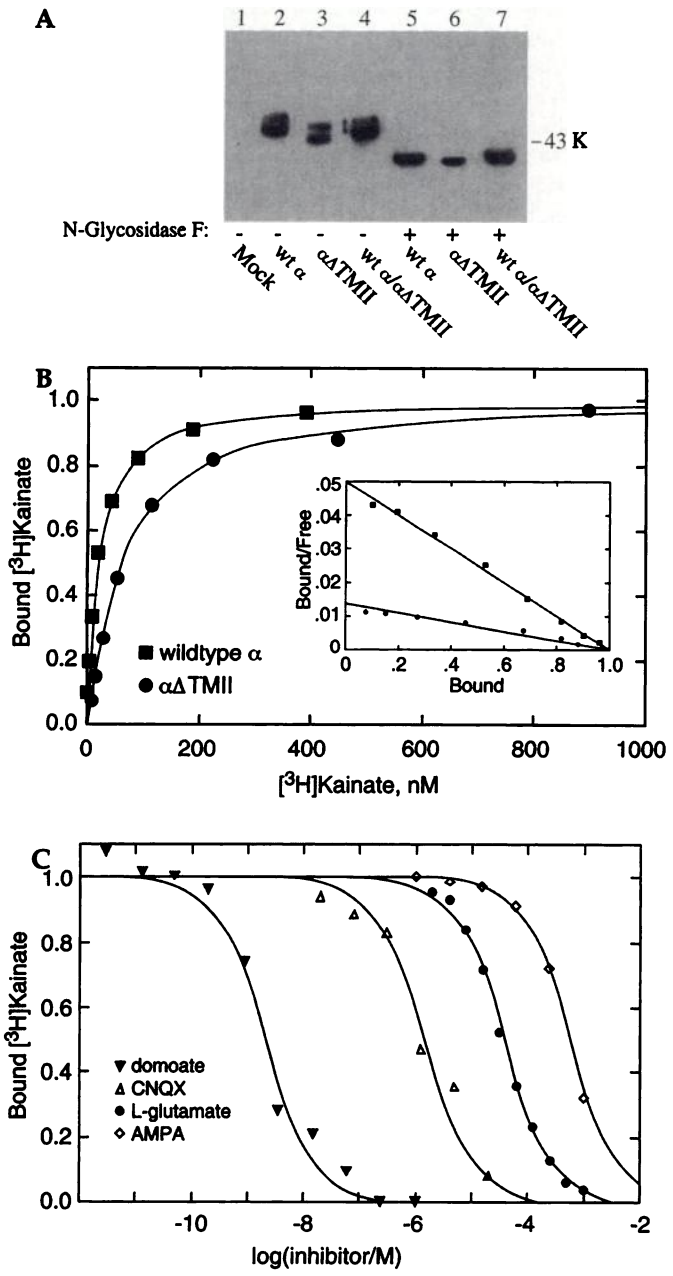

Fig. 2. A, Immunoblot of GFKARα with the deletion of "TMII" (αΔTMII) expressed in HEK 293 cells. Membrane preparations of the transfected HEK 293 cells were separated on 10% SDS-PAGE (under reducing conditions). *N*-Glycosidase F was used to remove *N*-linked oligosaccharides. Proteins were recognized by the specific antipeptide antibody (Ab-α1) and visualized by chemiluminescence. B, Equilibrium [^{3}H]kainate binding to αΔTMII expressed in HEK 293 cells. *Inset*, Scatchard plots derived from the saturation curve. The data for wild-type GFKARα are the same as those shown in Fig. 1. C, Displacement of [^{3}H]kainate (25 nM) binding to αΔTMII expressed in HEK 293 cells by glutamate analogs. Data are expressed as a percentage of specific binding in the absence of inhibitor. The K_I values calculated from the data shown in this figure are 1.5 nM for domoate, 1.1 μM for CNQX, 27 μM for L-glutamate, and 400 μM for AMPA.

differentially. Although GFKARα has two charged residues (E13 and R52) in these two motifs, GFKARβ has two uncharged residues (Q12 and A51) and relatively lower affinity for L-glutamate. To test whether charged residues introduced into these two sites of GFKARβ would affect ligand binding,

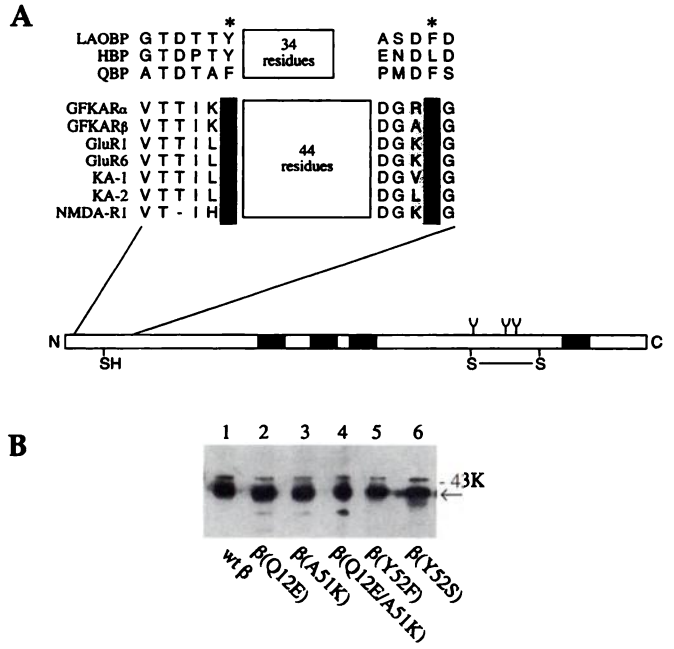

Fig. 3. A, Position of the GFKARβ mutants on the sequence and a comparison with the corresponding region of other glutamate receptors and bacterial periplasmic binding proteins according to the alignment of Sutcliffe *et al.* (31). *, Two residues in bacterial binding proteins that directly contact the ligand. B, Immunoblot of mutant receptor proteins of GFKARβ expressed in HEK 293 cells. Proteins were recognized using the GFKARβ-specific antibody Ab-β1 and visualized by chemiluminescence as described in Experimental Procedures.

subunits containing two single mutations (Q12E and A51K) and one double mutation (Q12E/A51K) were constructed and expressed in HEK 293 cells. The three mutants were expressed as efficiently as the wild-type GFKARβ as indicated by immunoblotting with Ab-β1 (Fig. 3B). Considering first [^{3}H]kainate binding (Fig. 4A), the mutant β(Q12E) exhibited an affinity similar to that of GFKARα (17 ± 1.4 nM) with positive cooperativity (n_H = 1.6 ± 0.3). In the case of the mutant β(A51K), affinity for [^{3}H]kainate is decreased (80 ± 8 nM) with little change in cooperativity (n_H = 1.5 ± 0.1). The affinity of the double-mutant β(Q12E/A51K) for kainate was slightly lower than that of wild-type GFKARβ (K_D = 40 ± 1 nM); however, no cooperativity in binding was observed. The effects of these mutations on L-glutamate binding (measured by the inhibition of [^{3}H]kainate binding) are more pronounced (Fig. 4B). β(Q12E) has increased affinity for L-glutamate (7.8 ± 1.2 versus 42 ± 0.3 μM for wild-type), but β(A51K) has drastically decreased affinity for L-glutamate (0.53 ± 0.17 mM). The double-mutant β(Q12E/A51K) has an affinity (25 ± 6 μM) intermediate between that of wild-type and that of the β(Q12E) mutant. These results showed that the negatively charged glutamate residue is very important for high affinity of kainate and L-glutamate, whereas the positively charged lysine residue is not necessarily associated with high affinity for kainate and L-glutamate. This is consistent with the fact that in KA-1 and KA-2, the homologous site of lysine is uncharged leucine and valine (41, 42).

Corresponding to the conserved tyrosine in the DGKYG motif, a phenylalanine residue in the bacterial periplasmic binding protein, lysine/arginine/ornithine binding protein (LAOBP), plays an important role in the binding of amino acids (43), and the homologous phenylalanine in NMDA re-

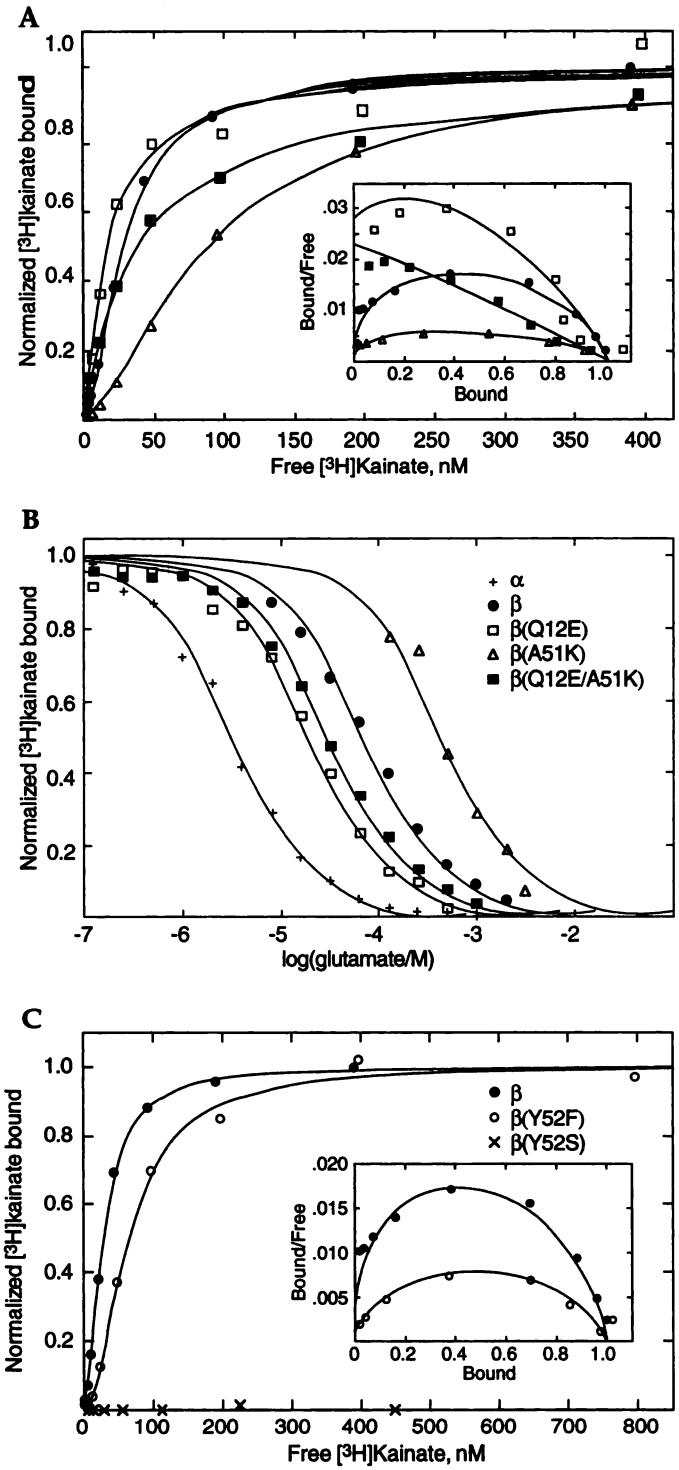

Fig. 4. A, Equilibrium binding of [^{3}H]kainate to mutants of GFKARβ expressed in HEK 293 cells. *Inset*, Scatchard plots of the saturation data. *Symbols* are defined in B. The data for GFKARβ are the same as shown for Fig. 1. B, Comparison of the competitive inhibition of [^{3}H]kainate binding by L-glutamate for mutants of GFKARβ expressed in HEK 293 cells. The membrane preparations were incubated with 20 nM [^{3}H]kainate and increasing concentrations of L-glutamate. The results are presented as a percentage of specific binding in the absence of L-glutamate. C, Equilibrium binding of [^{3}H]kainate to membrane preparations of HEK 293 cells transfected with wild-type GFKARβ and GFKARβ mutants, Y52F and Y52S.

ceptor (NR1) is important for glycine binding (30). Therefore, we mutated the tyrosine in GFKARβ to phenylalanine and serine (Y52F and Y52S). The phenylalanine mutant maintains the aromatic character but not the potential hydrogen bonding, whereas the serine mutant retains the hydroxyl group for potential hydrogen bonding but not the aromatic character. As shown in Fig. 3B, the expression levels for the two mutants were similar to that of wild-type GFKARβ; however, the binding characteristics differed dramatically. The β(Y52F) mutant had a 2-fold lower affinity for [^{3}H]kainate (K_D = 63.1 ± 2.7 nM, n_H = 1.8 ± 0.1; Fig. 4C) but no change in affinity for L-glutamate (K_I = 38 ± 2.5 μM; data not shown). Despite the fact that the β(Y52S) mutant was expressed as efficiently as wild-type β (Fig. 3B), [^{3}H]kainate binding was nearly abolished by the mutation. Some specific binding of both [^{3}H]kainate and [^{3}H]CNQX could be detected at ligand concentrations of >1 μM (data not shown), suggesting that the affinity is decreased by >100-fold for kainate and by >40-fold for CNQX. The facts that some binding can be detected and that the protein can be efficiently expressed suggest that the overall fold is probably maintained, although a significant structural reorganization cannot be ruled out. These results indicate that the aromatic ring of Y52 is crucial for generating a receptor capable of high affinity ligand binding.

DTT modulation of [^{3}H]kainate binding to goldfish cerebellar membranes. The reducing agent DTT has been shown to increase [^{3}H]kainate binding by 2–3-fold (12), suggesting the presence of a solvent-accessible disulfide bond or bonds. To gain insight into the underlying structural correlate (e.g., a disulfide bond), we characterized further the reaction of DTT on these receptor proteins. First, goldfish cerebellar membrane preparations, which are highly enriched in these two kainate receptors (12, 19), were treated with DTT (2 mM) at room temperature for 5 min, and the equilibrium binding of [^{3}H]kainate was measured. DTT increases [^{3}H]kainate equilibrium binding through the increase of affinity (K_D is decreased 2-fold) rather than the generation of cryptobinding sites (Fig. 5A). The association rate (k_{on}) of [^{3}H]kainate was too fast to be characterized in detail with a vacuum filtration assay (33). The dissociation rate (k_{off}) of [^{3}H]kainate from the kainate receptor rich membranes consists of two components (k_{off} = 0.07 and 0.006 sec^{-1}), each representing ~50% of the binding sites at 20 nM [^{3}H]kainate. DTT (2 mM) slowed both components by ~2-fold (Fig. 5B).

Treatment with combinations of DTT and other thioreactive agents were used to characterize the nature of the DTT enhancement of [^{3}H]kainate binding (Fig. 5C). The DTT enhancement of [^{3}H]kainate binding is persistent after removal of DTT from the membranes. This indicates that DTT does not directly affect the ligand-binding reaction and that the increase in [^{3}H]kainate binding is likely due to breaking of S—S bond or bonds by DTT. Cleavage of an S—S bond or bonds may affect either the conformation of the binding site (e.g., relative movement of the two extracellular domains in the process of binding a ligand) or the new free cysteines may directly contribute to kainate binding. To distinguish these possibilities, we tested the effect of the alkylating agent NEM (2 mM) on DTT enhancement of [^{3}H]kainate binding. NEM alone had no effect on [^{3}H]kainate binding. When NEM was applied after removal of DTT, the DTT-generated sulfhydryl

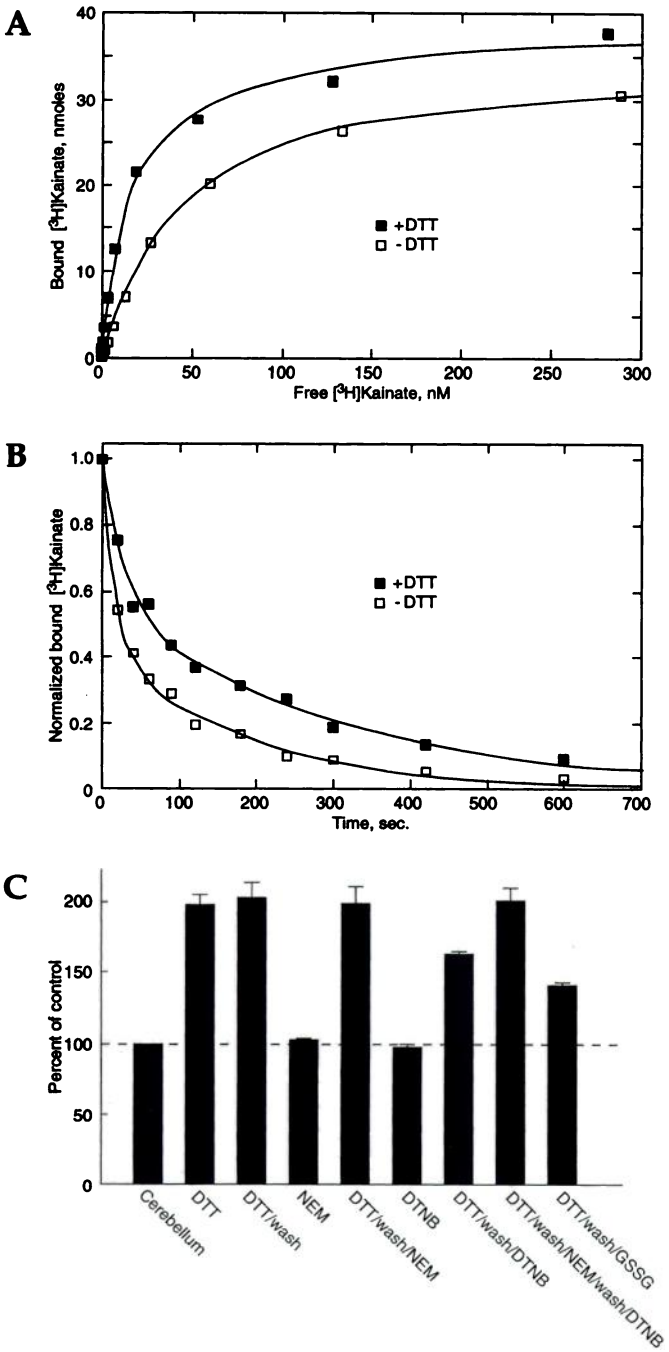

Fig. 5. A, Effects of DTT on equilibrium [^{3}H]kainate binding to kainate receptor-rich goldfish cerebellar membrane fragments. B, Effects of DTT on the dissociation of [^{3}H]kainate from goldfish cerebellar membrane fragments. Membrane fragments were incubated with 30 nM [^{3}H]kainate for 1 hr on ice. Excess unlabeled kainate (1 mM) was then added, and samples (500 μl) were assayed at the indicated times. C, Effects of thioreactive agents DTT, NEM, and DTNB on the equilibrium [^{3}H]kainate binding of goldfish cerebellar membrane fragments. [^{3}H]Kainate (25 nM) binding under different treatments is expressed as a percentage of the binding of nontreated samples.

groups were alkylated by NEM. No effect was observed on the DTT enhancement of [^{3}H]kainate binding, indicating that free thio-groups from the S—S bond are not directly involved in ligand binding. Two oxidizing agents, DTNB and GSSG, were used in an attempt to reform the putative disulfide bond. DTNB (0.2 mM) alone had no effect on [^{3}H]kainate binding. When applied after DTT treatment, DTNB partially reversed the DTT enhancement of [^{3}H]kainate binding, indicating that some of the free thio-groups could be reoxidized to a disulfide bond. This DTNB effect was completely blocked by pretreatment with 2 mM NEM. GSSG (3 mM) had the same effect as 0.2 mM DTNB (data not shown). We conclude that goldfish kainate receptors have solvent-accessible S—S bond or bonds and that the increase of affinity for kainate after DTT treatment is probably due to the cleavage of disulfide bond or bonds rather than a direct involvement of DTT or the thio-groups of cysteine residues in the binding interaction.

Equilibrium binding analysis of cysteine mutants of GFKARβ expressed in HEK cells. Like the native receptors from goldfish brain, cloned goldfish kainate receptors (GFKARα and GFKARβ) expressed in HEK 293 cells are also sensitive to DTT. [^{3}H]Kainate binding of the expressed GFKARα and GFKARβ was increased by 2 mM DTT to approximately the same level (150–200%) as the binding of native kainate receptors (compare Figs. 5C and 6C).

According to the current model for the transmembrane topology of kainate receptor proteins (25), three extracellularly located cysteine residues are present in each subunit (Fig. 3A). One is in the amino-terminal region, and the other two are located between TMIII and TMIV. These three cysteine residues are very conserved among members of the iGluR superfamily and are the likely candidates for the formation of the DTT-sensitive disulfide bonds. Each of the three cysteine residues (e.g., C27, C305, and C358) in GFKARβ was mutated to serine. All three cysteine mutants were expressed in transfected HEK 293 cells to a similar level as wild-type GFKARβ (Fig. 6A). Saturation binding analysis (Fig. 6B) showed that the affinity for β(C27S) was essentially unchanged (K_D = 37 ± 10 nM). On the other hand, both β(C307S) and β(C358S) mutants had increased affinity for [^{3}H]kainate (K_D = 9.0 ± 0.2 and 2.6 ± 0.2 nM, respectively). Thus, for both of these cysteine mutations, the affinity for [^{3}H]kainate was increased by >2-fold. Like wild-type GFKARβ, [^{3}H]kainate binding of the mutant β(C27S) was increased ~2-fold by 2 mM DTT (Fig. 6C). However, for the mutants β(C307S) and β(C358S), DTT no longer stimulated [^{3}H]kainate binding, and binding was unaffected by NEM and DTNB. The consequences of the mutations at positions 307 and 358 indicate that C307 and C358 form a solvent-accessible disulfide bond.

Kinetic analysis of wild-type and cysteine mutants of GFKARβ expressed in HEK cells. To characterize further the effects of the cysteine mutations, the dissociation of [^{3}H]kainate binding to membranes from transfected HEK 293 cells was studied. Wild-type GFKARβ exhibits a biphasic dissociation curve; the dissociation rate constant was ~0.02 sec^{-1} and was decreased ~2-fold by DTT (~0.009 sec^{-1}; Fig. 7A). The dissociation of [^{3}H]kainate from homomeric receptors formed from β(C27S) was decreased by DTT (0.028 versus 0.006 sec^{-1}; Fig. 7B). Clearly, the mechanism of binding is complex for both wild-type GFKARβ and β(C27S), and the increase in affinity in the presence of DTT is due, at least in part, to a slowing of the dissociation kinetics. Interestingly, dissociation of [3H]kainate became largely monophasic for both the β(C307S) and β(C358S) mutations (~0.0025 sec^{-1}; a faster component may have been present but represented <5% of the total binding; Fig. 7, C and D), and DTT had no effect on the dissociation kinetics. Thus, the DTT sensitivity

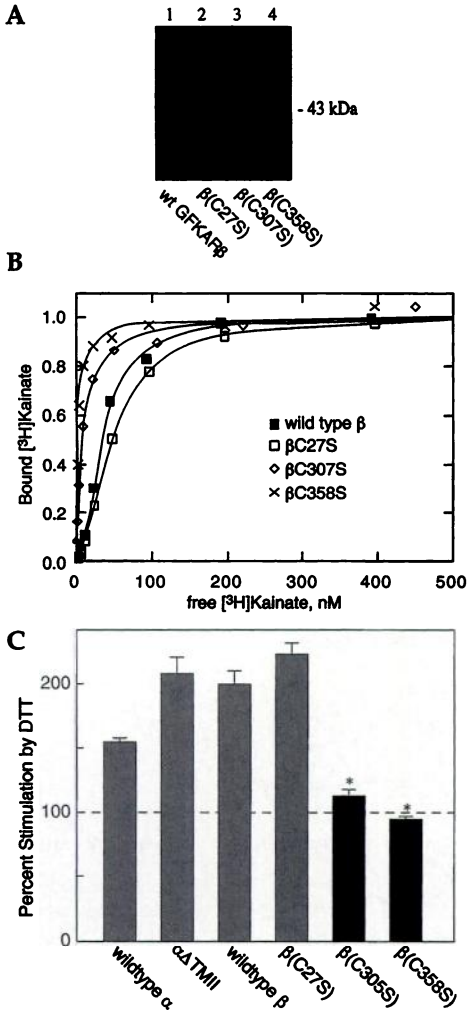

Fig. 6. A, Immunoblot of membranes from HEK 293 cells transfected with cysteine mutations of GFKARβ. B, Equilibrium [^{3}H]kainate binding to cysteine mutations of GFKARβ transiently expressed in HEK 293 cells. C, Effects of DTT on the [^{3}H]kainate binding to cysteine mutations of GFKARβ transiently expressed in HEK 293 cells. Membrane fragments were preincubated in HMEN buffer in the presence and absence of 2 mM DTT for 5 min. Equilibrium binding was with concentrations [^{3}H]kainate at the respective K_D value for each receptor. [^{3}H]Kainate binding is shown as a percentage of the binding in the untreated samples.

seems to arise from the cleavage of a disulfide bond between β(C307S) and β(C358S), and the dissociation kinetics are slowed by the loss of the disulfide.

Discussion

We have shown that two cloned goldfish kainate receptor subunits, GFKARα and GFKARβ (15), can be expressed effectively in transfected mammalian cells (HEK 293 cells). This study revealed several important features of goldfish kainate receptors. 1) [^{3}H]Kainate saturation binding analysis showed that GFKARα and GFKARβ have relatively similar affinities, although GFKARβ exhibited significant positive cooperativity that was absent in GFKARα. The affinities of GFKARα and GFKARβ for various glutamatergic ligands (L-glutamate, quisqualate, domoate, AMPA, and CNQX) were measured using a [^{3}H]kainate-binding inhibition assay. Although GFKARα and GFKARβ have similar affinities for domoate, CNQX, quisqualate, and AMPA, homomeric receptors formed from these two subunits showed a large difference (>30-fold) in the affinity for L-glutamate. 2) A deletion mutant (αΔTMII) of GFKARα, which lacks the segment previously thought to be the second-transmembrane domain (TMII), was efficiently expressed in transfected HEK 293 cells. This mutant was *N*-glycosylated in the same manner as the wild-type GFKARα and retained high affinity for kainate, indicating that kainate receptor subunit lacking the proposed "TMII," when expressed in transfected mammalian cells, can attain the wild-type topology and fold to form the ligand-binding site. 3) Mutation of three residues (Q12, A51, and Y52) in the amino-terminal extracellular region of GFKARβ indicates that they are important for ligand binding and may reside in the putative ligand-binding pocket, which is consistent with a three-dimensional structural model of non-NMDA receptors (31). 4) A solvent-accessible disulfide bond formed between two conserved cysteine residues in the second extracellular region was identified. The effect of this disulfide bond on ligand binding of the kainate receptor is consistent with the notion that iGluRs are modular proteins, in which ligand binding involves the movement of two large extracellular lobes (25).

Recent topological analysis of AMPA and kainate receptors showed that the amino-terminal region preceding TMI and the region between TMIII and TMIV are extracellular (15, 21, 23–26; Fig. 8). These two large extracellular regions are homologous to bacterial periplasmic amino acid-binding proteins (27, 28), a class of structurally and functionally well-characterized soluble proteins of the bacterial transport system. However, this proposed topology model is established only through indirect means (e.g., identification of *N*-glycosylation sites and proteolytic patterns), and it can be definitively proven only by solving the structure of the membrane protein. On the other hand, studies of the phosphorylation sites of kainate receptor GluR6 (44, 45) and AMPA receptor GluR1 (46, 47) suggest a different topology (48, 49). The expression and characterization of αΔTMII in this study are important in that they lend further evidence in support of a topology model with three-transmembrane segments. The "TMII" segment is clearly dispensable with regard to the overall folding and expression of the receptor proteins because αΔTMII protein was as efficiently expressed in transfected HEK 293 cells as wild-type GFKARα while retaining the *N*-glycosylation pattern and ligand-binding profiles of the wild-type GFKARα. This demonstrates further that the TMII segment is not a true transmembrane region. This is consistent with the recent finding that the two extracellular domains can be expressed as a soluble protein that retains high affinity ligand binding (50).

Consistent with the three-transmembrane topology model, analyses of the chimera between AMPA (GluR3) and kainate (GluR6) receptors (29) and mutations of NMDA receptor (NR1) (30) indicate that residues in both the first and second extracellular region are involved in ligand binding. Models of the extracellular ligand-binding domain of non-NMDA AMPA and kainate receptors have been presented based on homology with bacterial amino acid-binding proteins (31). Mutations and these models indicate a putative ligand-binding site formed partly by two conserved sequence motifs (VTTILE and DGKYG) in the amino-terminal region. In bacterial periplasmic binding proteins, residues in these two

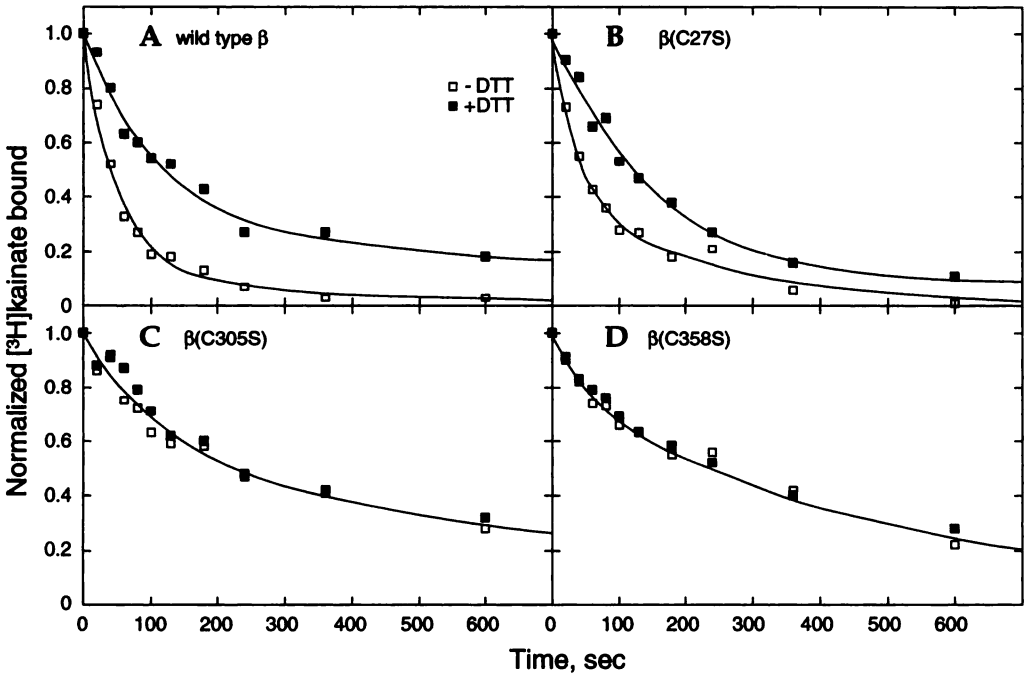

Fig. 7. Dissociation of [^{3}H]kainate from HEK 293 cell membranes expressing wild-type or cysteine mutants of GFKARβ in the presence or absence of 2 mM DTT.

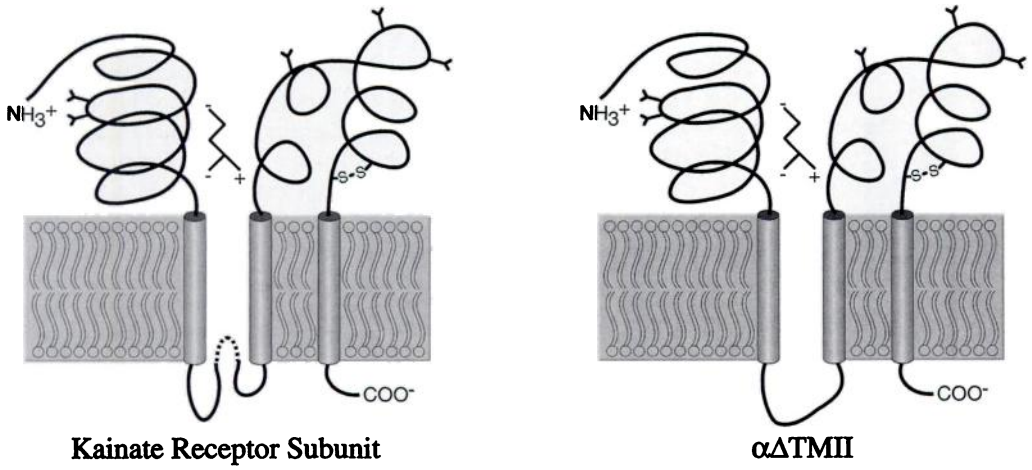

Fig. 8. Proposed transmembrane topology of kainate receptor subunit. *Dotted line*, TMII segment proposed to be associated with the ion channel. In the $\alpha\Delta$TMII mutation, this segment is deleted.

regions are important for ligand binding. Y14 of lysine/arginine/ornithine-binding protein (LAOBP) and HBP as well as F52 of LAOBP and L52 of HBP directly contact the ligand (38, 43, 51, 52). According to the alignment of Sutcliffe *et al.* (31), Y14 corresponds to the glutamate of VTTILE, and F52 corresponds to the tyrosine of DGKYG (28, 31). In both AMPA (39, 40) and NMDA (30) receptors, mutations of the position corresponding to glutamate (VTTILE) and lysine (DGKYG) in these two motifs affect ligand binding. However, the effects are more dramatic at the glutamate site than at the lysine site. A mutation of the lysine in DGKYG to glutamate decreases affinity for L-glutamate only 20-fold, and the effects of mutations at the lysine site have differential effects on channel activation by kainate and L-glutamate (39, 40).

Mutations of the three residues in GFKARβ in this study provide some additional information concerning the roles of this putative binding site. The effects of the β(Y52F) and β(Y52S) mutations indicate that the aromatic ring of Y32 was crucial for ligand binding. Removal of the hydroxyl group, as in the β(Y52F) mutant, marginally reduced the affinity for kainate but not for L-glutamate. However, replacement of the aromatic ring with a shorter chain, as in the β(Y52S) mutation, decreased affinity for kainate by >100-fold. This result is consistent with the role of the homologous F466 of NMDA receptor subunit NR1 (30). As mentioned above, the corresponding position in LAOBP and HBP directly contacts the ligand. GFKARβ has uncharged groups in both the glutamate and lysine positions (VTTIKQ and DGAYG) and binds L-glutamate with an affinity 30-fold less than that of GFKARα (VTTIKE and DGRYG). The addition of a negative charge to VTTILE (VTTIKQ to VTTIKE; Q12E mutant) increases the affinity, but the addition of a positive charge to DGKYG (DGAYG to DGKYG; A51K mutant) decreases the affinity. The double mutant has an affinity for L-glutamate between wild-type and the Q12E mutant. This effectively rules out the possibility that the lysine of DGKYG interacts with one of the negative charges of L-glutamate. Although other interpretations are possible, one plausible explanation is that the two conserved sequence motifs (VTTILE and DGKYG) are in proximity and the two charged residues interact directly. This is consistent with a homology model of kainate receptors (31), which is based on the struc-

ture of bacterial amino acid-binding proteins (51). Thus, the potential interaction of E12 and R51 of GFKARα could help determine the structure of the binding site by maintaining the proximity of the two loops. Glutamate (or glutamine in the case of GFKARβ) of the VTTILE motif would interact directly with the amine of L-glutamate. The tyrosine of DGKYG motif would then interact directly with the methylene groups of the L-glutamate side chain. The two residues (E12 and Y52), which correspond to residues that contact ligand in the bacterial proteins (Fig. 3), may also contact the ligand in GFKARβ. Finally, the lysine (or arginine) of the DGKYG motif could also interact electrostatically with E12. In this case, E12 would interact with both the positive charge of the ligand and the positive charge of the DGKYG motif. In GFKARβ, where position 12 is a glutamine, the A51K mutation would not be able to accommodate both the positive charge of the ligand and the positive charge introduced by the mutation.

Proteins with diverse biological functions have been shown to undergo a large hinged domain motion on ligand binding (53). The two large extracellular regions of kainate receptors not only are homologous to bacterial periplasmic amino acid binding proteins but also probably retain the salient structural features of these binding proteins; i.e., ligand binding involves the closure of two independent lobes. This notion is consistent with the effects on ligand binding of the cysteine mutations (C307S and C358S) of GFKARβ and the deletion mutation of GFKARα ($\alpha\Delta$TMII). Two cysteine residues, located in the loop between two transmembrane segments (TMIII and TMIV), are conserved in all of the members of iGluR superfamily. In the case of goldfish kainate receptors, DTT treatment resulted in a decrease in the dissociation rate of kainate. The β(C305S) and β(C358S) mutants have increased affinity and decreased dissociation rate for kainate; both are no longer sensitive to DTT, indicating that C305 and C358 form this DTT-sensitive disulfide bond. This is consistent with the finding that two cysteine residues (C744 and C798) at the homologous positions of the NMDA receptor (NR1) mediate redox effect on channel activity (54, 55). Because these two cysteine residues are absolutely conserved among members of the iGluR family, this proposed disulfide bond may be a common structural feature present in all iGluRs. Our modeling suggests that the disulfide bond in this position may restrict the closure of the two lobes on agonist binding (31). Perhaps the cleavage of the disulfide leads allows the two lobes to close with fewer restrictions in the bound form, resulting in the decreased rate of dissociation of kainate.

The four cloned and expressed nonmammalian kainate receptors (frog KBP, chick KBP, and goldfish GFKARα and GFKARβ) all show physiologically meaningful affinities for L-glutamate (K_D = 1–70 μM). The concentration of L-glutamate in the synapse shifts between 1 μM under resting conditions and 1 mM at its peak (56). The physiological role of these nonmammalian vertebrate kainate receptors is still not clear because ion channel activity has yet to be demonstrated for wild-type receptors in heterologous expression systems. The possibility exists, however, that suitable conditions for the reconstitution of the potential ion channel activity have not been found in these expression systems. Nevertheless, kainate receptors have been implicated in the process of synapse formation in the avian brain, as indicated by the finding that kainate receptor expression was significantly induced by an imprint stimulus in the duckling hyperstriatum ventral (13). In case of the orphan receptor GluRδ, although heterologously expressed GluRδ shows no ligand-binding activity and no ion channel activity, GluRδ has important physiological roles in the cerebellum parallel-fiber/Purkinje cell synapses as shown by a transgenic experiment (6). Alternatively, to understand their physiological role in nonmammalian vertebrate brain, the overall synaptic architecture and characteristics may need to be taken into consideration. It is noteworthy that the binding of glutamate to the glutamate transporter, instead of the actual reuptake of glutamate, affects the clearance kinetics of glutamate in the synaptic cleft (57–59). The above features of the glutamate synapse raise the possibility that in addition to possible ion channel activity, nonmammalian vertebrate kainate receptors might also affect the clearance of the neurotransmitter L-glutamate.

Acknowledgments

We thank Dr. David R. Hampson (University of Toronto) for generously providing monoclonal antibody KAR-B1, Dr. Michael Sutcliffe (University of Leicester) for useful discussions and generation of the homology models, and Dr. G. A. Weiland for critical reading of the manuscript.

References

1. Monaghan, D. T., R. J. Bridges, and C. W. Cotman. The excitatory amino acid receptors: their classes, pharmacology, and distinct properties in the function of the central nervous system. *Annu. Rev. Pharmacol. Toxicol.* **29**:365–402 (1989).
2. Nakanishi, S., and M. Masu. Molecular diversity and functions of glutamate receptors. *Annu. Rev. Biophys. Biomol. Struct.* **23**:319–348 (1994).
3. Seeburg, P. H. The molecular biology of mammalian glutamate receptor channels. *Trends Neurosci.* **16**:359–365 (1993).
4. Hollmann, M., and S. Heinemann. Cloned glutamate receptors. *Annu. Rev. Neurosci.* **17**:31–108 (1994).
5. Lomeli, H., R. Sprengel, D. J. Laurie, G. Kohr, A. Herb, P. H. Seeburg, and W. Wisden. The rat *delta*-1 and *delta*-2 subunits extend the excitatory amino acid receptor family. *FEBS Lett.* **315**:318–322 (1993).
6. Kashiwabuchi, N., K. Ikeda, K. Araki, T. Hirano, K. Shibuki, C. Takayama, Y. Inoue, T. Kutsuwada, T. Yagi, Y. Kang, S. Aizawa, and M. Mishina. Impairment of motor coordination, Purkinje cell synapse formation, and cerebellar long-term depression in GluRδ mutant mice. *Cell* **81**:245–252 (1995).
7. Ottiger, H. P., A. Gerfin-Moser, F. Del Principe, F. Dutly, and P. Streit. Molecular cloning and differential expression patterns of avian glutamate receptor mRNAs. *J. Neurochem.* **64**:2413–2426 (1995).
8. Ueda, H., and V. Hieber. Down-regulation of AMPA-type glutamate receptor gene expression during goldfish optic nerve regeneration. *Mol. Brain Res.* **32**:151–155 (1995).
9. Kurosawa, N., K. Kondo, N. Kimura, T. Ikeda, and Y. Tsukada. Molecular cloning and characterization of avian N-methyl-D-aspartate receptor type 1 (NMDA-R1) gene. *Neurochem. Res.* **19**:575–580 (1994).
10. Hampson, D. R., and R. J. Wenthold. A kainic acid receptor from frog brain purified using domoic acid affinity chromatography. *J. Biol. Chem.* **263**: 2500–2505 (1988).
11. Gregor, P., N. Eshhar, A. Ortega, and V. Teichberg. Isolation, immunochemical characterization and localization of the kainate subclass of glutamate receptor from chick cerebellum. *EMBO J.* **7**:2673–2679 (1988).
12. Ziegra, C. J., J. M. Willard, and R. E. Oswald. Biochemical characterization of kainate receptors from goldfish brain. *Mol. Pharmacol.* **42**:203–209 (1992).
13. Kimura, N., N. Kurosawa, K. Kondo, and Y. Tsukada. Molecular cloning of the kainate-binding protein and calmodulin genes which are induced by an imprinting stimulus in ducklings. *Mol. Brain Res.* **17**:351–355 (1993).
14. Gregor, P., I. Mano, I. Maoz, M. McKeown, and V. Teichberg. Molecular structure of the chick cerebellar kainate-binding subunit of a putative glutamate receptor. *Nature (Lond.)* **342**:689–692 (1989).
15. Wo, Z. G., and R. E. Oswald. Transmembrane topology of two kainate receptor subunits revealed by N-glycosylation. *Proc. Natl. Acad. Sci. USA* **91**:7154–7158 (1994).
16. Wada, K., C. J. Dechesne, S. Shimasaki, R. G. King, K. Kusano, A. Buonanno, D. R. Hampson, C. Banner, R. J. Wenthold, and Y. Nakatani.

Sequence and expression of a frog brain complementary DNA encoding a kainate-binding protein. *Nature (Lond.)* **342**:684–689 (1989).
17. Dechesne, C. J., M. D. Oberdorfer, D. R. Hampson, K. D. Wheaton, A. J. Nazarali, G. Goping, and R. J. Wenthold. Distribution of a putative kainic acid receptor in the frog central nervous system determined with monoclonal and polyclonal antibodies: evidence for synaptic and extrasynaptic localization. *J. Neurosci.* **10**:479–490 (1990).
18. Somogyi, P., N. Eshhar, V. I. Teichberg, and J. D. Roberts. Subcellular localization of a putative kainate receptor in Bergmann glial cells using a monoclonal antibody in the chick and fish cerebellar cortex. *Neuroscience* **35**:9–30 (1990).
19. Ziegra, C. J., R. E. Oswald, and A. H. Bass. [^{3}H]Kainate localization in goldfish brain: receptor autoradiography and membrane binding. *Brain Res.* **527**:308–317 (1990).
20. Eshhar, N., C. Hunter, R. J. Wenthold, and K. Wada. Structural characterization and expression of a brain specific gene encoding chick kainate binding protein. *FEBS Lett.* **297**:257–262 (1992).
21. Wo, Z. G., and R. E. Oswald. A topological analysis of goldfish kainate receptors predicts three transmembrane segments. *J. Biol. Chem.* **270**: 2000–2009 (1995).
22. Wo, Z. G., and R. E. Oswald. Asn265 of frog kainate binding protein is a functional glycosylation site: implications for the transmembrane topology of glutamate receptors. *FEBS Lett.* **368**:230–234 (1995).
23. Bennett, J. A., and R. Dingledine. Topology profile for a glutamate receptor: three transmembrane domains and a channel-lining re-entrant membrane loop. *Neuron* **14**:373–384 (1995).
24. Hollmann, M., C. Maron, and S. Heinemann. N-Glycosylation site tagging suggests a three transmembrane domain topology for the glutamate receptor GluR1. *Neuron* **13**:1331–1343 (1994).
25. Wo, Z. G., and R. E. Oswald. Unraveling the modular design of glutamate-gated ion channels. *Trends Neurosci.* **18**:161–168 (1995).
26. Wood, M. W., H. M. A. VanDongen, and A. M. J. VanDongen. Structural conservation of ion conduction pathways in K channels and glutamate receptors. *Proc. Natl. Acad. Sci. USA* **92**:4882–4886 (1995).
27. Nakanishi, N., N. A. Schneider, and R. Axel. A family of glutamate receptor genes: evidence for the formation of heteromultimeric receptors with distinct channel properties. *Neuron* **5**:569–581 (1990).
28. O'Hara, P. J., P. O. Sheppard, H. Thøgersen, D. Venezia, B. A. Haldeman, V. McGrane, K. M. Houamed, C. Thomsen, T. L. Gilbert, and E. R. Mulvihill. The ligand-binding domain in metabotropic glutamate receptors is related to bacterial periplasmic binding proteins. *Neuron* **11**:41–52 (1993).
29. Stern-Bach, Y., B. Bettler, M. Hartley, P. O. Sheppard, P. J. O'Hara, and S. F. Heinemann. Agonist selectivity of glutamate receptors is specified by two domains structurally related to bacterial amino acid-binding proteins. *Neuron* **13**:1345–1357 (1994).
30. Kuryatov, A., B. Laube, H. Betz, and J. Kuhse. Mutational analysis of the glycine-binding site of the NMDA receptor: structural similarity with bacterial amino acid-binding proteins. *Neuron.* **12**:1291–1300 (1994).
31. Sutcliffe, M. J., Z. G. Wo, and R. E. Oswald. Three-dimensional models of non-NMDA glutamate receptors. *Biophys. J.* **70**:1575–1589 (1996).
32. Lee, B. S., R. B. Gunn, and R. R. Kopito. Functional differences among nonerythroid anion exchangers expressed in a transfected human cell line. *J. Biol. Chem.* **266**:11448–11454 (1991).
33. Henley, J. M., and R. E. Oswald. Solubilization and characterization of kainate receptors from goldfish brain. *Biochim. Biophys. Acta* **937**:102–111 (1988).
34. Willard, J. M., and R. E. Oswald. Interaction of the frog brain kainate receptor expressed in Chinese hamster ovary cells with a GTP-binding protein. *J. Biol. Chem.* **267**:19112–19116 (1992).
35. Cheng, Y., and W. H. Prusoff. Relationship between the inhibition constant (K_I) and the concentration of inhibitor which causes 50 per cent inhibition (I_{50}) of an enzymatic reaction. *Biochem. Pharmacol.* **22**:3099–3108 (1973).
36. Hampson, D. R., K. D. Wheaton, C. J. Dechesne, and R. J. Wenthold. Identification and characterization of the ligand binding subunit of a kainic acid receptor using monoclonal antibodies and peptide mapping. *J. Biol. Chem.* **264**:13329–13335 (1989).
37. Ziegra, C. J., J. M. Willard, and R. E. Oswald. Coupling of a purified goldfish brain kainate receptor with a pertussis toxin-sensitive G protein. *Proc. Natl. Acad. Sci. USA* **89**:4134–4138 (1992).
38. Wolf, A., E. W. Shaw, B. H. Oh, H. De Bondt, A. K. Joshi, and G. F. Ames. Structure/function analysis of the periplasmic histidine-binding protein: mutations decreasing ligand binding alter the properties of the conformational change and of the closed form. *J. Biol. Chem.* **270**:16097–16106 (1995).
39. Uchino, S., K. Sakimura, K. Nagahari, and M. Mishina. Mutations in a putative agonist binding region of the AMPA-selective glutamate receptor channel. *FEBS Lett.* **308**:253–257 (1992).
40. Li, F., N. Owens, and T. A. Verdoorn. Functional effects of mutations in the putative agonist binding region of recombinant α-amino-3-hydroxy-5-methyl-4-isoxazolepropionic acid receptors. *Mol. Pharmacol.* **47**:148–154 (1995).
41. Werner, P., M. Voigt, K. Keinänen, W. Wisden, and P. H. Seeburg. Cloning of a putative high-affinity kainate receptor expressed predominantly in hippocampal CA3 cells. *Nature (Lond.)* **351**:742–744 (1991).
42. Herb, A., N. Burnashev, P. Werner, B. Sakmann, W. Wisden, and P. H. Seeburg. The KA-2 subunit of excitatory amino acid receptors shows widespread expression in brain and forms ion channels with distantly related subunits. *Neuron* **8**:775–785 (1992).
43. Oh, B. H., G. F. Ames, and S. H. Kim. Structural basis for multiple ligand specificity of the periplasmic lysine-, arginine-, ornithine-binding protein. *J. Biol. Chem.* **269**:26323–26330 (1994).
44. Raymond, L. A., C. D. Blackstone, and R. L. Huganir. Phosphorylation and modulation of recombinant GluR6 glutamate receptors by cAMP-dependent protein kinase. *Nature (Lond.)* **361**:637–641 (1993).
45. Wang, L. Y., F. A. Taverna, X. P. Huang, J. F. MacDonald, and D. R. Hampson. Phosphorylation and modulation of a kainate receptor (GluR6) by cAMP-dependent protein kinase. *Science (Washington D. C.)* **259**:1173–1175 (1993).
46. Nakazawa, K., S. Mikawa, T. Hashikawa, and M. Ito. Transient and persistent phosphorylation of AMPA-type glutamate receptor subunits in cerebellar Purkinje cells. *Neuron* **15**:697–709 (1995).
47. Yakel, Y. L., P. Vissavajjhala, V. A. Derkach, D. A. Brickey, and T. R. Soderling. Identification of a Ca^{2+}/calmodulin-dependent protein kinase II regulatory phosphorylation site in non-N-methyl-D-aspartate glutamate receptors. *Proc. Natl. Acad. Sci. USA* **92**:1376–1380 (1995).
48. Roche, K. W., L. A. Raymond, C. Blackstone, and R. L. Huganir. Transmembrane topology of the glutamate receptor subunit GluR6. *J. Biol. Chem.* **269**:11679–11682 (1994).
49. Taverna, F. A., L. Y. Wang, J. F. MacDonald, and D. R. Hampson. A transmembrane model for an ionotropic glutamate receptor predicted on the basis of the location of asparagine-linked oligosaccharides. *J. Biol. Chem.* **269**:14159–14164 (1994).
50. Kuusinen, A., M. Arvola, and K. Keinänen. Molecular dissection of the agonist binding site of an AMPA receptor. *EMBO J.* **14**:6327–6332 (1995).
51. Oh, B. H., J. Pandit, C. H. Kang, K. Nikaido, S. Gokcen, G. F. L. Ames, and S. H. Kim. Three dimensional structure of the periplasmic lysine/arginine/ornithine-binding protein with and without a ligand. *J. Biol. Chem.* **268**: 11348–11355 (1993).
52. Oh, B. H., C. H. Kang, H. De Bondt, S. H. Kim, K. Nikaido, A. K. Joshi, and G. F. Ames. The bacterial periplasmic histidine-binding protein: structure/function analysis of the ligand-binding site and comparison with related proteins. *J. Biol. Chem.* **269**:4135–4143 (1994).
53. Gerstein, M., A. M. Lesk, and C. Chothia. Structural mechanisms for domain movement in proteins. *Biochemistry* **33**:6739–6749 (1994).
54. Gozlan, H., and Y. Ben-Ari. NMDA receptor redox sites: are they targets for selective neuronal protection? *Trends Pharmacol. Sci.* **16**:368–374 (1995).
55. Sullivan, J. M., S. F. Traynelis, H. S. V. Chen, W. Escobar, S. F. Heinemann, and S. A. Lipton. Identification of two cysteine residues that are required for redox modulation of the NMDA subtype of glutamate receptor. *Neuron* **13**:929–936 (1994).
56. Nicholls, D., and D. Attwell. The release and uptake of excitatory amino acids. *Trends Pharmacol. Sci.* **11**:462–468 (1990).
57. Wadiche, J. I., J. L. Arriza, S. G. Amara, and M. P. Kavanaugh. Kinetics of a human glutamate transporter. *Neuron* **14**:1019–1027 (1995).
58. Tong, G., and C. E. Jahr. Block of glutamate transporters potentiates postsynaptic excitation. *Neuron* **13**:1195–1203 (1994).
59. Barbour, B., B. U. Keller, I. Llano, and A. Marty. Prolonged presence of glutamate during excitatory synaptic transmission to cerebellar Purkinje cells. *Neuron* **12**:1331–1343 (1994).

Send reprint requests to: Robert E. Oswald, Ph.D., Department of Pharmacology, College of Veterinary Medicine, Cornell University, Ithaca, NY 14853. E-mail: reo1@cornell.edu